

# Modeling of Fluorescence Sources within Tissue using Angular Domain Imaging

Rongen L. K. Cheng, Polly Tsui, Glenn H. Chapman, Nick Pfeiffer, and Bozena Kaminska  
Simon Fraser University, School of Engineering Science, 8888 University Drive,  
Burnaby, B.C., Canada V5A 1S6

## INTRODUCTION

Fluorescence imaging has been researched increasingly in recent years as a potential tool for screening and diagnosing precancerous cells, and managing premalignant lesions.<sup>1</sup> Fluorophores are triggered when an excitation light source is absorbed and an emission light source is resulted. The excitation source is specific on the targeting fluorophores, and the excitation wavelength can be eliminated by a simple filter in the imaging system. However, biological tissue samples are highly scattering, and current fluorescence imaging methods are not considering the amount of noise due to the scattered photons. Only a small amount of photons traverse through the tissue samples unaffected. These are the ballistic and quasi-ballistic photons carrying information about the imaged subject. This paper focuses on expanding our research to compare imaging the surface to detect the fluorescence pattern by applying the Angular Domain Imaging to enhance the scattering filtration.<sup>2</sup> We investigate the feasibility of Angular Domain Imaging (ADI) in two different fluorescence situations: point sources simulating the artificially inserted fluorophores and plane source simulating the naturally occurred fluorophores.

## FLUORESCENCE IMAGING

Fluorescence is the emission of light of a longer wavelength after absorbing the light source at a different wavelength. This shift in the fluorescence excitation and emission spectra is referred to as the Stokes Shift. By studying the autofluorescing cells in tissue over time, abnormal or cancerous behaviors can be detected and observed. Fluorophores can be naturally found in tissue or artificially inserted. Collagen is a commonly found fluorophores approximately 1mm underneath the epidermis with an excitation spectrum of 340-470nm and an emission spectrum of 420-540nm. On the other hand, fluorescence chemical such as R6G, with an excitation spectrum at 533nm and an emission spectrum between 555-585nm, can be inserted into samples artificially. In this research paper, Monte Carlo simulations are used to demonstrate the effectiveness

of applying ADI on both naturally and artificially occurring fluorophores.

## ANGULAR DOMAIN IMAGING

Angular Domain Imaging is an optical tomography method that accepts only photons within a narrow range of exit angles. The principle behind the ADI is that photons scatter in a nearly uniform angular distribution are significantly removed by the angular filter, while ballistic and quasi-ballistic photons remain close to their original trajectory and are detected. By eliminating the scattered light, images can be constructed with the information carried by the ballistic and quasi-ballistic photons without the noise created by the scattered photons.<sup>3,4</sup>

The angular filter using in this experiment is the linear collimating array. By aligning the array of collimators with the trajectory of the ballistic photons, all scattered photons with an exit angle greater than the predefined acceptance angle. Figure 1 shows the basic setup of the linear collimating array. ADI is especially suited in fluorescence imaging compared to other optical tomography methods such as optical coherence tomography. ADI is independent on both coherent and wavelength and works well when the scattering is modest.

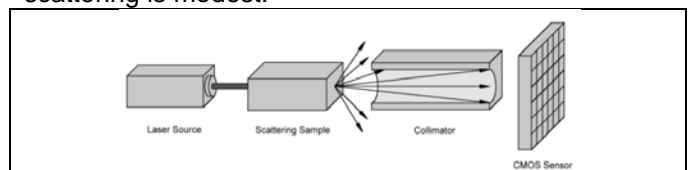


Figure 1 - Angular Domain Imaging configuration

In the previous paper, we have compared the detection of a series of point fluorescence sources using simple surface imaging with a camera, ADI filter using a collimating array, ADI filter using a spatiofrequency filter.<sup>2</sup> We have compared the surface distribution of light from a series of point sources. The initial scattering surface showed in figure 2(a) has a widely distributed source across the area. The surface when using a simple camera system as in figure 2(b) removes some of the scattered light and imaging by using a spatiofrequency lens ADI system as in figure 2(c). For a collimating array in figure 2(d),

significantly rejects scattered light and leaving almost only ballistic and quasi-ballistic photons. These results suggest that the collimating array is the best method with the fluoresce situation which we will explore further in this paper.<sup>2</sup> Furthermore, the collimating array shows significant improvement than conventional fluorescence imaging using a simple camera system.

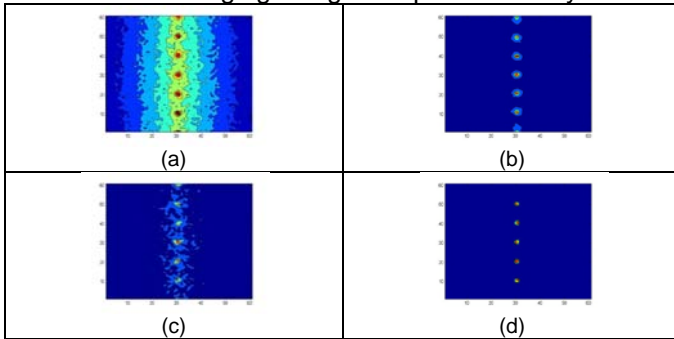


Figure 2 - Contour maps of simulation results with scattering thickness of 2mm (a) at scattering medium surface (b) simple 50mm converging lens. (c) SFF with acceptance angle of  $2.5^\circ$  (d) linear collimating array with aspect ratio of 10:1

### MONTE CARLO SIMULATION SETUP

Two simulation scenarios of fluorescing situations are constructed in the Monte Carlo program: emissions from point sources at regular intervals to emulate the artificially inserted fluorophores, and emission from a uniform source with non emitting areas to model the autofluorescence of collagen in tissues. For the point source emission simulation, six photon sources at  $100\ \mu\text{m}$  intervals each emitting 5 million photons are placed behind a scattering medium with thicknesses ranging from 1mm to 2mm. For the uniform emission simulations, a uniformly lit background emitting with 60 million photons is placed beneath the same scattering medium. A linear collimating array with different aspect ratios is placed immediately after the scattering medium with the collimating holes set at  $25\ \mu\text{m}$  radius on  $100\ \mu\text{m}$  centers and various lengths from  $250\ \mu\text{m}$  to  $1000\ \mu\text{m}$ . An additional test with a 50mm lens placed at twice the lens' focal distance to model the image sensor setup needed to capture an image in real life. The scattering medium has a scattering coefficient of  $200\text{cm}^{-1}$ , a g factor of 0.85, an index of refraction of 1.33, and various thicknesses which is the typical value for collagen detection through skin.

### SIMULATION RESULTS – POINT SOURCE EMISSIONS

In general, using a point source emission for the simulation is to emulate the optical behavior when

performing ADI with artificially injected fluorophores. This technique provides us information about the optical behavior of tissue by measuring the output intensity in various spot within a tissue which assists us to identify potential structural absorber within the tissue.

The thicknesses for modeling the biological tissue are 1mm, 1.5mm, and 2mm. This range of thickness corresponds to the location of collagen, a natural fluorophores, which is approximately 1mm underneath the epidermis. The reason for selecting these thicknesses is that typical depth required for physicians to identify irregular tissues, such as tumors, are mostly lying on the top layers of the tissues. Furthermore, we will try to discover the imaging limitation with current proposed ADI technique. In previous research<sup>2</sup>, we demonstrated that we are able to use the collimator holes arrays to filter out scattered photons and retrieve the photon sources location at various tissue thicknesses. In figure 2, we aligned the point source directly with the collimator holes with successful results; we now investigate shifting the point sources away from the collimator holes to verify the performance of the imaging system.

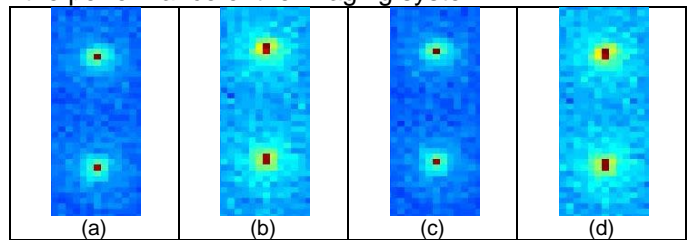


Figure 3 - Contour maps of point sources at various positions from the center of scattering medium surface (a) original Position (b)  $25\ \mu\text{m}$  to the right (c)  $50\ \mu\text{m}$  to the right (d)  $25\ \mu\text{m}$  to the left

Figure 3 shows the simulation results at the scattering medium surface. Figure 3(a) shows the point sources are positioned directly to the collimator holes and Figure 3(b), (c), (d) show vertically and horizontally shifted photon sources. It clearly shows that there is a slightly different optical pattern between these configurations. While fixing the position of the collimator holes array, we expect the total number of photons pass through would be different. Figure 4 shows the angular domain filtered results where the collimator holes arrays are placed directly on top of the scattering surface to eliminate the effect from reflective index changing between the medium and air. These results show that we are able to image the point sources clearly with the collimator holes array. Although the number of photons passing through the collimator holes is reduced with shifted point sources from 544 in figure 4(a) to 154 in figure 4(c), the overall

image quality remains constant as the high intensity point indicates the locations of the point sources.

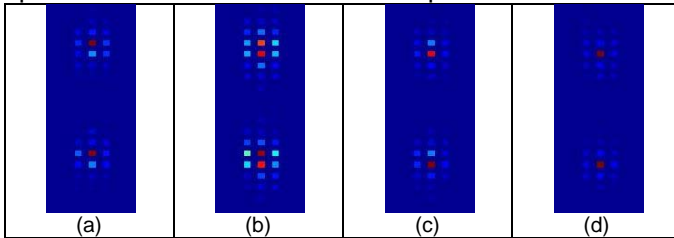


Figure 4 - Contour maps of point sources at various positions from the center of collimator holes (a) aligned with collimator holes (b) 25µm to the right of the collimator holes (c) 50µm from or in between collimator holes (d) 25µm to the left of the collimator holes

Table 1 - Maximum number of photons detected after collimator from point sources at various positions.

Position of Point Source Relative to Collimator Holes	Maximum Number of Photons Detected	% of Photon Intensity Reduction
aligned	544	0
25 µm to the right	362	33.5
between 2 holes	154	71.7
25 µm to the left	356	34.5

Table 1 summarizes the difference in the maximum number of photons between photon point source positions. It shows that the reduction due to shifted sources is roughly 70% to 30%. These peak photon locations remain a respectable value for the camera sensor to pick up the signals. When placing a 3-row collimator arrays right after the scattering medium, figure 4 shows the center spots of the point source and the 'ring' effect around the center spot. If the fluorescence is not a true point source, the effect of this shifting will be reduced. These results suggest that with a modest aspect ratio of 10:1 with modest scattering thickness of up to 2mm, we can readily identify fluorescence point sources through tissue.

### SIMULATION RESULTS – LAMBERTIAN PLANE SOURCE EMISSIONS

Now let us consider the effect of large area fluorescence emitter combine with ADI. We switched the point source into a uniform plane emitting surface with different widths of absorbing/non-emitting areas to simulate the situation of collagen in tissue with damaged non-fluorescing areas.

In this simulation, we created a Lambertian plane source with horizontal absorbers lying across the surface. The absorbers have an initial width of 200µm with 1mm spacing between each absorber, as show in figure 5(a). Then, the photons pass through the scattering medium with thickness of 1mm or 1.5mm.

Figure 5 (b) shows the image plane at the surface of the scattering medium with 1mm thickness. It shows that we are not able to see any absorbers within the image, as the number of scattered photons dominates to the image. As mentioned previously, collimator holes reject scattering photons with acceptance angle based on its aspect ratio. Figure 5(c) has 10:1 aspect ratio with acceptance angle of 5.72° where the dark areas are detectable. Figure 5(d) has 20:1 aspect ratio with acceptance angle of 2.86°. We can see that the increase of aspect ratio allows us to see the pattern of absorbers. Then, placing a 50mm converging lens to transmit the collimator array image to a detector, the quality of imaging the absorbers increases. This is as we expected because the simple camera setup further reduces the number of scattered photons as the scattered photons diverge away from the center of its original position.

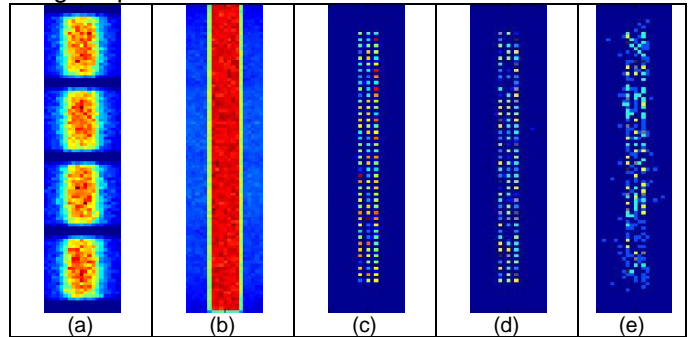


Figure 5 - Contour maps of plane source at various positions (a) Before entering the scattering medium (b) After scattering medium with 1mm thickness (c) Collimator holes with 10:1 aspect ratio (d) Collimator holes with 20:1 aspect ratio (e) 200mm away from the collimator holes with 50mm lens placed in between

As the thickness of the medium increases from 1mm to 1.5mm, the number of scattered photons increases exponentially based on the Beer-Lambert law. Therefore, the number of ballistic and quasi-ballistic photons will reduce which disintegrates the image. Figure 6(c) and (d) again show the angular domain filtered images with the different acceptance angles. Comparing these images with figure 5(c) and (d), the intensity of the image for the high scattered medium reduces. The reduction rate for the number of photons pass through the collimator holes with different aspect ratio decreases as the number of ballistic and quasi-ballistic photons remains but the number of scattered photons reduces gradually as shown in table 2. With 1.5mm scattering medium, the percentage reduction of the number photons pass through the filter decreases by 19.7%. This increase is due to the thicker medium and the collimator holes reject these scattered photons.

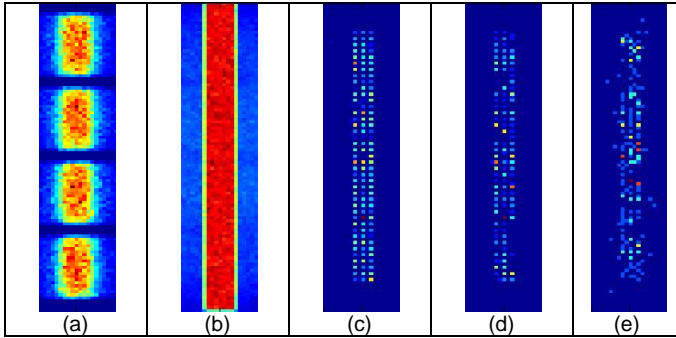


Figure 6 - Contour maps of plane source at various positions (a) Before entering the scattering medium (b) After scattering medium with 1.5mm thickness (c) Collimator holes with 10:1 aspect ratio (d) Collimator holes with 20:1 aspect ratio (e) 200mm away from the collimator holes with 50mm lens placed in between

Table 2 – Total number of photons detected after different collimator aspect ratio and medium thickness.

Medium Thickness	Collimator Holes Aspect Ratio	Total Number of Photons Detected	% of Photon Intensity Reduction
1.0mm	5:1	23028	0
	10:1	3750	83.7
	15:1	1959	91.5
	20:1	1323	94.3
1.5mm	5:1	18498	19.7
	10:1	2361	89.7
	15:1	1113	95.2
	20:1	681	97.1

Next, we increase the width of the absorber from 200 $\mu$ m to 400 $\mu$ m with 1mm spacing between each absorber. This allows us to verify that scattering medium thickness and absorber size correlate to the resolution limit of the system. The assumption is based on the travel path Lambertian photon source where the photon at the edge of the absorber will propagate through the scattering medium and will enter through the collimator holes. As a result, the image captured after the collimator holes contains these edge scattered photons. By increasing the absorber size, we are reducing the edging effect of the scattered photons. Figure 7(a) shows the plane at the Lambertian source with 400 $\mu$ m absorbers. Immediately, we can see the 3 horizontal lines compare the 5 horizontal lines in figure 6(a). In figure 7(b), we increase the absorbers size and remain unable to detect the absorber directly at the scattering medium. With 10:1 aspect ratio, we start to see the dark area within the image (figure 7(c)). And when we increase the aspect ratio to 20:1, we clearly able to detect the dark area. Adding the lens into this system improves even further as in figure 7(e). This clearly shows that increasing the absorbing area size while keeping the thickness the same increases the detectability with the collimator aspect ratio rises rapidly from 200 $\mu$ m to 400 $\mu$ m.

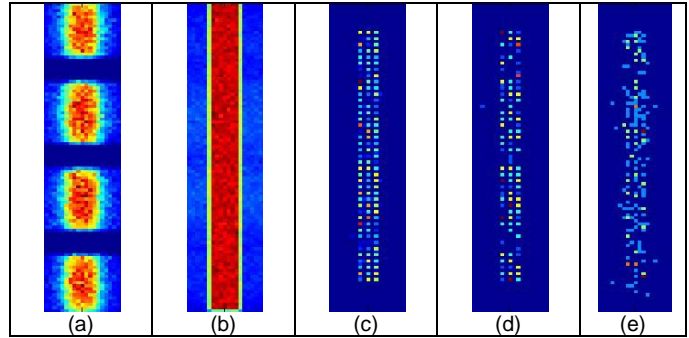


Figure 7 - Contour maps of plane source with 400 $\mu$ m absorbers at various positions (a) Before entering the scattering medium (b) After scattering medium with 1.5mm thickness (c) Collimator holes with 10:1 aspect ratio (d) Collimator holes with 20:1 aspect ratio (e) 200mm away from the collimator holes with 50mm lens placed in between

## CONCLUSION

The simulations indicate that collimating arrays with modest aspect ratios work well in detecting fluorescence in shallow depths at tissue scattering levels. When using point sources, we can detect them with depth up to 2mm, independent of location. Also, we can image the filtrated image with a simple camera setup. With uniform sources, collimator array shows that with 10:1 and 20:1 aspect ratio, can image absorbers up to 200 $\mu$ m width at 1mm depth. As absorbing area increase, image resolution increases, and adding a lens to image the collimating array enhance the detection even further.

## REFERENCE

1. Slaughter, D. P., Southwick, H. W., and Smejkal, W. "Field cancerization in oral stratified squamous epithelium; clinical implications of multcentric origin." *Cancer* 6 (1953): 963-968.
2. Tsui, P., Cheng, R., Chiang, G., Chapman, G. H., Kaminska, B., and Pfeiffer, N.,. "Spatiofrequency Filters for Imaging Fluorescence in Scattering Media." *Proc. SPIE Photonics West* 7562, no. 75620B (2010).
3. Chapman, G. H., Trinh, M., Pfeiffer, N., Chu, G., and Lee, D. "Angular Domain Imaging of Objects Within Highly Scattering Media using Silicon Micromachined Collimating Arrays." *IEEE J. Special Topics on Quantum Electronics* 9, no. 2 (2003): 257-266.
4. Chapman, G. H., Tank, M. S., Chou, G., and Trinh, M. "Optical imaging of objects within highly scattering mediums using Silicon Micromachined Collimating Arrays." *Proc. SPIE Photonics West* 4616 (2002): 187-198.